Amino Acids (2014) 46:2333–2343
DOI 10.1007/s00726-014-1780-5

ORIGINAL ARTICLE

Efficacy of the designer antimicrobial peptide SHAP1 in wound healing and wound infection

Da Jung Kim · Young Woong Lee · Myung Keun Park · Ju Ri Shin · Ki Jung Lim · Ju Hyun Cho · Sun Chang Kim

Received: 28 November 2013 / Accepted: 5 June 2014 / Published online: 22 June 2014

Abstract Infected wounds cause delay in wound closure and impose significantly negative effects on patient care and recovery. Antimicrobial peptides (AMPs) with antimicrobial and wound closure activities, along with little opportunity for the development of resistance, represent one of the promising agents for new therapeutic approaches in the infected wound treatment. However, therapeutic applications of these AMPs are limited by their toxicity and low stability in vivo. Previously, we reported that the 19-amino-acid designer peptide SHAP1 possessed salt-resistant antimicrobial activities. Here, we analyzed the wound closure activities of SHAP1 both in vitro and in vivo. SHAP1 did not affect the viability of human erythrocytes and keratinocytes up to 200 μM, and was not digested by exposure to proteases in the wound fluid, such as human neutrophil elastase and *Staphylococcus aureus* V8 proteinase for up to 12 h. SHAP1 elicited stronger wound closure activity than human cathelicidin AMP LL-37 in vitro by inducing HaCaT cell migration, which was shown to progress via transactivation of the epidermal growth factor receptor. In vivo analysis revealed that SHAP1 treatment accelerated closure and healing of full-thickness excisional wounds in mice. Moreover, SHAP1 effectively countered *S. aureus* infection and enhanced wound healing in *S. aureus*-infected murine wounds. Overall, these results suggest that SHAP1 might be developed as a novel topical agent for the infected wound treatment.

Keywords Antimicrobial peptides · SHAP1 · Wound healing · Infected wound treatment · Protease resistance · Cytotoxicity

D. Jung Kim · Y. W. Lee · M. K. Park · J. R. Shin · K. J. Lim · S. C. Kim (✉)
Department of Biological Sciences, Korea Advanced Institute of Science and Technology, 291 Daehak-ro, Yuseong-gu, Daejeon 305-701, Republic of Korea
e-mail: sunkim@kaist.ac.kr

J. H. Cho (✉)
Department of Biology, Research Institute of Life Science, Gyeongsang National University, 501 Jinju Dae-ro, Jinju 660-701, Republic of Korea
e-mail: juhyun.cho@gnu.ac.kr

Introduction

The skin functions as a physical barrier against microbial pathogens. Once this physical barrier is disrupted by wounding, however, microbial pathogens can gain access to tissues (Torpy et al. 2005). Invasion of these microbial pathogens leads to wound infection by degrading or damaging tissues through the production of a variety of enzymes and toxins, which causes delay in wound closure (Gopinath et al. 2005). Thus, infected wounds impose significantly negative effects on patient care and recovery (Bowler 2002). To treat wound infections, several antibiotic drugs such as chloramphenicol, gentamicin, neomycin, and bacitracin are applied topically on open sores; however, the routine use of topical antibiotics leads to the progressive decline of therapeutic efficacies of these antibiotics due to antimicrobial resistance (McHugh et al. 2011; Myhrman et al. 2012; Lipsky and Hoey 2009). Therefore, there is a strong need for the development of new classes of drugs for the infected wound treatment.

One potential source of novel topical agents for the infected wound treatment is antimicrobial peptides (AMPs), which constitute a major component of the ancient, non-specific innate defense system in most

multicellular organisms, forming the first line of defense against invading microbes (Kim et al. 2013). AMPs are short (<50 amino acids), amphipathic molecules with hydrophobic and cationic amino acids (Hancock and Sahl 2006; Ma et al. 2012). Unlike conventional antibiotics, which operated on specific intracellular targets, many AMPs physically and rapidly permeate and destroy the bacterial membrane or essential components inside the cells. Thus, the chances of developing AMP resistance by target modification are slim (Mookherjee and Hancock 2007). Although these peptides were initially characterized for their direct antimicrobial activities, there is an increasing appreciation for the immunomodulatory activities of AMPs. The immunomodulatory activities of AMPs, especially human cathelicidin AMP LL-37 and β-defensins (hBDs), are extremely diverse and include, but are not limited to, the stimulation of epithelial cell migration, promotion of angiogenesis, and suppression of pro-inflammatory response (Koczulla et al. 2003; Mookherjee et al. 2006; Shaykhiev et al. 2005; Niyonsaba et al. 2007). LL-37 and hBDs also play important roles in wound closure, by promoting cell migration and proliferation (Tokumaru et al. 2005; Niyonsaba et al. 2007). For example, LL-37 has been shown to enhance the migration of keratinocytes and human corneal epithelial cells via epidermal growth factor receptor (EGFR) transactivation (Yin and Yu 2010; Carretero et al. 2008). In case of hBDs, they elicited intracellular Ca^{2+} mobilization, and increased the migration and proliferation of keratinocytes and human umbilical vein endothelial cells (Baroni et al. 2009). Owing to their multiple functions, including antimicrobial and wound closure activities, LL-37 and hBDs are considered promising agents for new therapeutic approaches in the infected wound treatment. However, therapeutic applications of these AMPs have been hindered by several problems, such as toxicity and low stability in vivo (Marr et al. 2006; Hawrani et al. 2008; De Zotti et al. 2012). Many AMPs are toxic to mammalian cells at higher concentrations due to their membrane lytic mechanism (Shin et al. 2013). In fact, LL-37 has shown nonselective cell toxicity and hemolytic activity, and causes DNA fragmentation in cell cultures (Steinstraesser et al. 2009). hBD-3 also showed high cytotoxicity after gene transfer to primary keratinocyte cell cultures (Steinstraesser et al. 2008). Moreover, LL-37 and hBDs generally have low stability in vivo. The antimicrobial activities of LL-37 and hBDs are strongly antagonized under physiological salt concentrations (Overhage et al. 2008; Park et al. 2004). It has been also reported that these AMPs are susceptible to degradation by both endogenous human proteases and proteases secreted from pathogens. For example, LL-37 is destroyed by human neutrophil elastase and V8 proteinase secreted by *Staphylococcus aureus*, which is a major cause of infection in injured patients (Pasupuleti et al. 2009; Sieprawska-Lupa et al. 2004).

Desired characteristics of a novel therapeutic for the infected wound treatment would include a broad-spectrum antimicrobial activity, low cytotoxicity, and strong wound closure activity that is capable of withstanding the host environment, including high salt concentration and proteases. Recently, we screened a series of 32 synthetic peptides for improved structural stability and high antimicrobial activity under the physiological conditions. These peptides were composed of a core motif in which cationic amino acid residues and hydrophobic amino acid residues are located in an alternating pattern, with the two capping motifs APKAM and LQKKGI introduced, respectively, into the N- and C-terminal ends thereof, which form an amphipathic α-helix. The capping motifs were introduced to ensure structural stability of the secondary structure of the entire peptide irrespective of surrounding salt concentration, thus giving rise to an increase in the antimicrobial activity of the peptides under high salt concentration (Kim et al. 2008; Park et al. 2004). Among them, SHAP1 (APKAMKLLKKLLKLQKKGI) showed a potent antimicrobial activity against bacteria and fungi, and maintained its activity in the presence of 200 mM NaCl. In the current work, we have expanded on the characterization of SHAP1 and demonstrated that it also promotes wound closure both in vitro and in vivo.

Materials and methods

Biological materials

Blood drawn from healthy volunteers was used for preparation of human erythrocytes. HaCaT cells were kindly provided by Dr. J.H. Choi (Korea Advanced Institute of Science and Technology, Daejeon, Korea) (Choi et al. 2012) and were cultured in Dulbecco's modified Eagle's medium (DMEM) containing 10 % fetal bovine serum (FBS) and 1 % penicillin/streptomycin. All cell culture media and reagents were purchased from Lonza (Basel, Switzerland). Antibodies raised against phospho-EGFR, EGFR, phospho-signal transducer and activator of transcription (STAT) 3, STAT3 and α-tubulin were purchased from Cell Signaling Technology, Inc. (Danvers, MA, USA). Anti-rabbit IgG was obtained from Amersham Pharmacia Biotech, Inc. (Piscataway, NJ, USA).

Peptides and enzymes

The synthetic peptides, SHAP1 and LL-37 (LLGDFF RKSKEKIGKEFKRIVQRIKDFLRNLVPRTES), were synthesized by Anygen (Kwangju, Korea). Synthesized

peptides were purified to over 95 % by reversed-phase high-pressure liquid chromatography (HPLC) on a Delta-Pak C18 column (3.9 mm × 300 mm, Waters, Milford, MA, USA). The peptide content of lyophilized samples was determined by quantitative amino acid analysis with a Pico-tag system on a Beckman 121 MB amino acid analyzer (Beckman Coulter, Fullerton, CA, USA). Human neutrophil elastase and *S. aureus* V8 proteinase were obtained from Calbiochem (La Jolla, CA, USA) and Bio-Col GmbH (Potsdam, Germany), respectively.

Hemolysis and in vitro cytotoxicity assay

Hemolysis activity was assayed as described by Jang et al. (2012). Briefly, 3 ml of freshly prepared human erythrocytes was washed with isotonic phosphate-buffered saline (PBS), pH 7.4, until the color of the supernatant turned clear. The washed erythrocytes were then diluted to a final volume of 20 ml with the same buffer. Ten microliters of peptide samples, serially diluted in PBS, were added to 190 µl of the cell suspension in microcentrifuge tubes. Following gentle mixing, the tubes were incubated at 37 °C for 30 min and then centrifuged at 4,000×*g* for 5 min. Aliquots of 100 µl of supernatant were diluted to 1 ml with PBS and absorbance at 567 nm was measured to monitor the release of hemoglobin, which indicated erythrocyte membrane damage. Zero hemolysis and 100 % hemolysis were determined in PBS and 0.2 % Triton X-100, respectively. The percentage of hemolysis was calculated using the following equation: Hemolysis $(\%) = (A_s - A_0)/(A_{100} - A_0) \times 100$, where A_s is the absorbance of the sample, A_{100} is the absorbance of completely lysed erythrocytes in 0.2 % Triton X-100, and A_0 is the absorbance in the complete absence of hemolysis.

To analyze in vitro cytotoxicity, HaCaT cells were cultured in 96-well plates (10^4 cells/well) in DMEM with 10 % FBS. After 24 h of incubation, cells were treated with each peptide (0–200 µM) and incubated for another 24 h. The cytotoxicity test was performed using a lactate dehydrogenase (LDH) release-based assay kit purchased from Roche Applied Science (Mannheim, Germany) according to the manufacturer's instructions. Controls were performed with 0.2 % Triton X-100 and set as 100 % LDH release. The relative LDH release is defined by the ratio of LDH released over total LDH in the intact cells. Less than 10 % LDH release were regarded as non-toxic effect level in our experiments. All samples were run in triplicate and the experiments were repeated at least three times independently.

Resistance to proteolytic digestion

Protease resistance of the peptides (SHAP1 and LL-37) was assessed by sodium dodecyl sulfate–polyacrylamide gel electrophoresis (SDS-PAGE) analysis. To test whether the peptides were digested by proteases, 5 µg of each peptide was incubated with human neutrophil elastase (0.3 µg, 29 units/mg) or *S. aureus* V8 proteinase (0.1 µg, 2,000 mU), respectively, in the digestion buffer (100 mM Tris–HCl, pH 7.5, 50 mM NaCl) at 37 °C. At the designated timepoints, the digestion mixture was sampled and analyzed by 16.5 % tricine-SDS-PAGE.

Cell migration assay

Cell migration was evaluated using a Boyden chamber assay (Neuroprobe, Cabin John, MD, USA), as described previously (Tokumaru et al. 2005). Designated amounts of SHAP1 or LL-37 were added to the bottom wells of a 48-well Boyden chamber (Neuro Probe, Gaithersburg, MD, USA), and a polyvinylpyrrolidone-free polycarbonate membrane (8 µm; Neuro probe, Gaithersburg, MD, USA) was placed on the wells. The membrane was precoated with 0.5 % gelatin (Sigma-Aldrich, St. Louis, MO, USA) at room temperature for 1 h and then washed extensively with PBS. Subconfluent HaCaT cells were harvested with trypsin–EDTA (0.05 % trypsin and 0.5 mM EDTA) and resuspended in DMEM without 10 % FBS at 10^5 cells/ml. A 50-µl aliquot of the HaCaT cells (5×10^3 cells/well) was added to the upper wells, and the chamber was incubated at 37 °C in a humidified atmosphere of air with 5 % CO_2 for 6 h. The cells that adhered to the upper surface of the membrane were removed by scraping with a rubber blade, and the cells that moved through the membrane and stayed on the lower surface of the membrane were considered to be migrated cells. The membrane was fixed with methanol for 15 min and then stained with hematoxylin and eosin (Sigma-Aldrich, St. Louis, MO, USA). The membrane was then mounted between two glass slides with 90 % glycerol, and the number of migrated cells was quantified using five random microscopic fields (magnification ×400) per filter. Each experiment was repeated at least three times independently.

Cell proliferation assay

HaCaT cells were seeded onto 96-well plates (Nunc, Penfield, NY, USA) at a density of 10^4 cells/well in 0.1 ml of DMEM supplemented with 10 % FBS, and allowed to attach overnight. The medium was removed and replaced with serum-free DMEM, and cells were treated with serially diluted peptide samples (final concentrations ranging 0.25–16 µM) and incubated for another 24 h. Cell proliferation was measured by a 3-(4,5-dimethylthiazol-2-yl)-2,5-diphenyl tetrazolium bromide (MTT) assay using the CellTiter 96-cell proliferation assay kit (Promega, Madison, WI, USA). The percentage of cell proliferation was

determined using the following equation: Relative cell proliferation (%) = $(A_s - A_0)/(A_c - A_0) \times 100$, where A_s is the absorbance of the sample, A_c is the absorbance of control (PBS) and A_0 is the background absorbance. Each experiment was repeated at least three times independently.

Scratch wound closure assay

In vitro wound closure was assayed in confluent cell monolayers as described (Radek et al. 2009). HaCaT cells were seeded in 6-well plates (Nunc, Penfield, NY, USA) and grown until they reached confluence (48 h). In some experiments, HaCaT cells were grown to 60 % confluence, followed by EGFR-specific small interfering RNA (siRNA) treatment using the G-fectin transfection reagent (Genolution Pharmaceuticals, Inc., Seoul, Korea) for 24 h to interrupt the expression of cellular EGFR. Cells were starved for 12 h in DMEM without 10 % FBS and then scratched once vertically with a 200-μl pipette tip to create an artificial wound. After being washed twice to remove cellular debris by PBS, cells were treated with SHAP1 or LL-37. PBS was used as a negative control. Cells were photographed before peptide treatment ($t = 0$ h) and 24 h after peptide treatment ($t = 24$ h) using an inverted phase contrast microscope (Carl Zeiss, Irvine, CA, USA). Same fields of images were captured, and the wound areas were estimated by Adobe Photoshop® v.5.0 (Adobe, San Jose, CA, USA). Relative closure was calculated as $(X_0 - X_{24h})/(C_0 - C_{24h})$, where X_0 = width of the scratch at time 0, X_{24h} = width of the scratch after 24 h exposure to the peptide, C_0 = width of the scratch at time 0, and C_{24h} = width of the scratch after 24 h exposure to the control (PBS). Each experiment was repeated at least three times independently.

Western blot analysis

Cells were lysed with 10× lysis buffer (Cell Signaling Technology, Danvers, MA, USA). Protein concentration in the extracts was determined with a bicinchoninic acid (BCA) assay (Pierce, Rockford, IL, USA). 150 μg of protein was separated on a 10 % SDS-PAGE gel and transferred to polyvinylidene difluoride membrane (Amersham Pharmacia Biotech, Inc., Piscataway, NJ, USA). The membranes were probed with antibodies specific to phospho-EGFR, EGFR, phospho-STAT3, STAT3, or α-tubulin. The membranes were then treated with horseradish peroxidase-conjugated donkey anti-rabbit IgG and developed by an enhanced chemiluminescence (ECL) detection reagent (Amersham Pharmacia Biotech, Inc., Piscataway, NJ, USA) according to the manufacturer's protocol. All experiments were performed on three separate occasions, with representative blots shown.

Animal model

Female BALB/c mice (8 weeks old) were purchased from Samtako (Osan, Korea). All mice were housed in cages under specific pathogen-free conditions, and given water and standard laboratory chow ad libitum during the experiments. Mice were anesthetized by an intraperitoneal injection of ketamine (1.2 mg/animal; Fort Dodge Animal Health, Fort Dodge, IA) and xylazine (0.25 mg/animal; Miles Inc., Shawnee, KS, USA). A full-thickness 10-mm punch biopsy wound was made on the back of each mouse as previously reported (Lee et al. 2004; Philp et al. 2003). The wounds were topically treated with 50 μl of 1 μM SHAP1, 0.25 μM LL-37, or PBS (vehicle control) every 24 h by pipetting the liquid directly onto the wound area ($n = 5$ animals per group). Each wound site was then digitally photographed at the indicated time intervals, and wound areas were determined on photographs using Adobe Photoshop® v.5.0. Changes in wound areas over time were expressed as the percentage of the original wound areas.

For bacterial inoculation, *S. aureus* (ATCC 29213) was used. A 2-cm^2 area of the back of each mouse was shaved and the skin was disinfected with ethanol. Single punch biopsies were performed on the back of the mice, resulting in 2-mm-diameter full-thickness wounds. Each wound was inoculated with 5 μl of PBS containing 5×10^5 CFU of *S. aureus*. Starting 24 h later, 10 μl of 1 μM SHAP1 or PBS was topically applied every 24 h ($n = 5$ animals per group). On day 3 after infection, tissue was collected and fixed in 10 % buffered formalin. The samples were sectioned and stained with hematoxylin and eosin and visualized by light microscopy. This experiment was performed twice. All procedures were approved by the Animal Care and Use Committee of Korea Advanced Institute of Science and Technology.

Assessment of wound infection

Tissue samples harvested on day 3 after infection were homogenized in 1.5 ml of PBS. Serially diluted aliquots of homogenates were cultured on selective medium for *S. aureus* (mannitol salt agar; Sigma-Aldrich, St. Louis, MO, USA) after incubation for 18 h at 37 °C, and the number of CFU/g tissue was subsequently calculated.

Statistical analysis

Values from groups were compared using a Student's *t*-test. Differences were considered significant when p was <0.001.

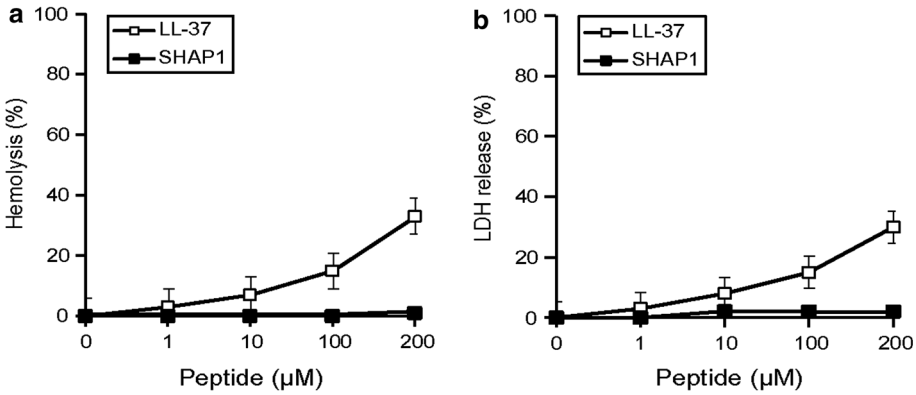

Fig. 1 Cytotoxicity of SHAP1 against human cells. **a** Hemolytic activity. A fresh human erythrocyte suspension was incubated with each peptide. Release of hemoglobin into the supernatant was monitored to indicate membrane damage of erythrocytes. **b** In vitro cytotoxicity. Each peptide was added to HaCaT cells. After 24 h of incubation with each peptide, cell viability was measured by the LDH assay. Data in (**a**) and (**b**) represent the mean ± SD of three independent experiments performed in triplicate

Results

Cytotoxicity of SHAP1 against human cells

Earlier experiments disclosed that a number of AMPs exhibit various levels of lytic activity toward mammalian cells (Mookherjee and Hancock 2007). Notably, LL-37 is cytotoxic to normal eukaryotic cells and exhibits a significant degree of hemolytic activity (Steinstraesser et al. 2009). For a peptide to be of pharmaceutical interest, high therapeutic activities must be combined with low toxicity against normal host cells. Therefore, we assessed the cytotoxicity of SHAP1 by hemolysis assay (Fig. 1a) and LDH assay using HaCaT cells (Fig. 1b). The cytotoxicity of SHAP1 was compared with LL-37. The results showed that, in accordance with the previous results (Malmsten et al. 2011), LL-37 showed significant toxic effect at high concentrations. LL-37 lysed 33.1 % of erythrocytes (Fig. 1a), and yielded 30.4 % LDH release at 200 μM, indicating a disruption of HaCaT cells (Fig. 1b). On the other hand, SHAP1 did not show any toxicity against erythrocytes and HaCaT cells at all tested concentrations.

Protease resistance of SHAP1

One of the major limitations of AMPs for the infected wound treatment is inactivation by both endogenous human proteases and proteases secreted from invading microbes in the wound site. To test the protease resistance of SHAP1, SHAP1 was incubated with human neutrophil elastase or *S. aureus* V8 proteinase for up to 12 h and the digestion mixtures were analyzed by tricine-SDS-PAGE. As shown in Fig. 2, SHAP1 was not digested at all by both proteases up to 12 h. We also conducted the same experiment with LL-37 as a control. In contrast to SHAP1, LL-37 was cleaved to small fragments by human neutrophil elastase as early as 1 min. LL-37 was also cleaved by 4 h of incubation with *S. aureus* V8 proteinase.

Efficacy of SHAP1 on in vitro wound closure

Migration and proliferation of human keratinocytes are critical factors that contribute to efficient wound closure. Therefore, we tested the capacity of SHAP1 to induce migration and proliferation of HaCaT cells. In these experiments, LL-37 was included as a control. We first investigated whether SHAP1 induced HaCaT cell migration using a Boyden chamber assay (Fig. 3a). Various amounts of peptides and cultured HaCaT cells were added to the lower and upper chambers, respectively. After incubation for 6 h, the migrated cells were counted. In SHAP1-treated cells, a dose-dependent increase in cell migration was observed over a concentration from 0 to 1.5 μM, with optimal migration at 1 μM. SHAP1 induced a 4.5-fold increase in cell migration compared with the control treatment (PBS), which is approximately two times more potent than LL-37 (2.2-fold increase at 0.25 μM). Next, we assessed the influence of SHAP1 on HaCaT cell proliferation by a MTT assay. As shown in Fig. 3b, no noteworthy differences were found in cell proliferation between HaCaT cells treated with SHAP1 at all test concentrations (up to 16 μM) and control cells (PBS). The proliferation of HaCaT cells was unaffected by LL-37 in accordance with the previous results (Carretero et al. 2004, 2008). High concentrations of LL-37 rather inhibited the growth of HaCaT cells. Overall, these results suggested that SHAP1 promotes wound closure by inducing HaCaT cell migration.

To confirm this possibility, a scratch wound closure assay was used to assess the potential effect of SHAP1 on

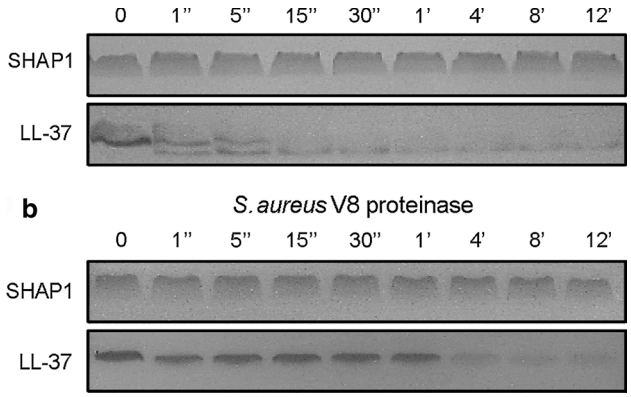

Fig. 2 Protease resistance of SHAP1. Each peptide was incubated with human neutrophil elastase (**a**) and *S. aureus* V8 proteinase (**b**) in the digestion buffer at 37 °C. At the designated timepoints, the digestion mixture was sampled and analyzed by 16.5 % tricine-SDS-PAGE

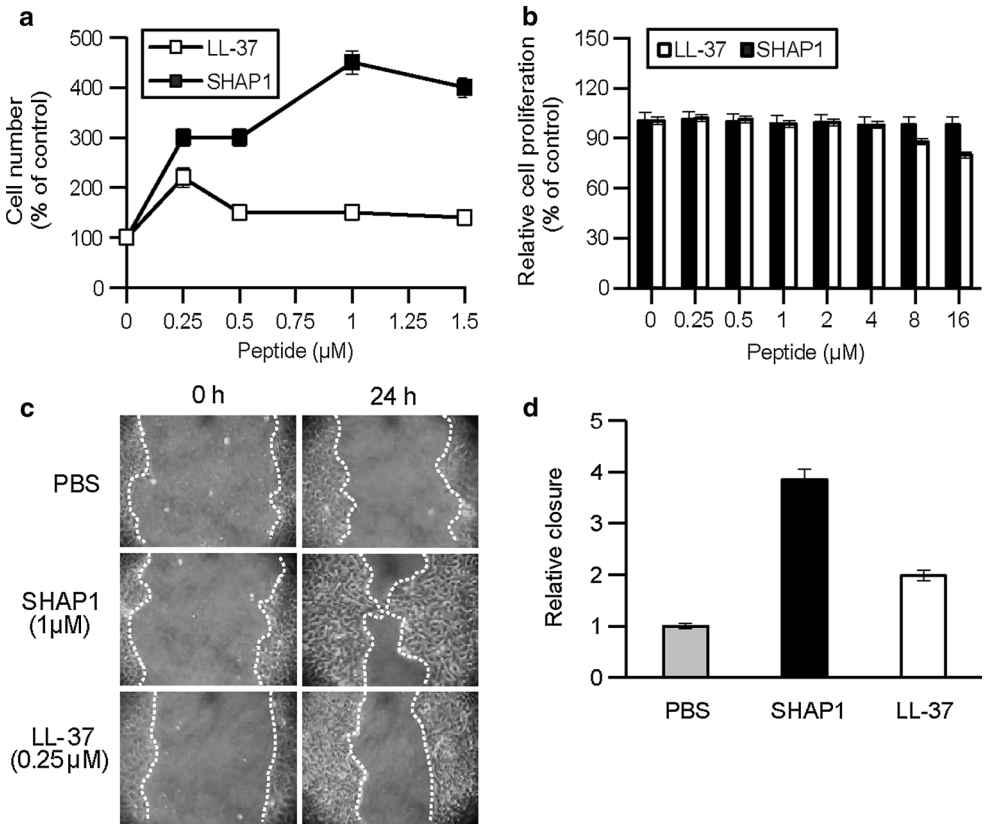

Fig. 3 Stimulating effect of SHAP1 on in vitro wound closure. **a** SHAP1-induced cell migration. HaCaT cell migration-inducing activity of SHAP1 was analyzed with a Boyden chamber assay. Indicated amounts of SHAP1 or LL-37 were added to the lower wells of a 48-well Boyden chamber. After HaCaT cells were added to the upper wells and incubated for 6 h, the migrated cells were counted. **b** SHAP1-induced cell proliferation. After incubation for 24 h with indicated amounts of SHAP1, cell viability was assessed using a MTT assay. Data in **a** and **b** represent the mean ± SD of three independent experiments performed in triplicate. **c**, **d** SHAP1-induced wound closure in HaCaT cells. In vitro wound closure was assessed using a scratch wound closure assay. HaCaT cells were grown to confluence on culture plates. Cells were serum-starved for 12 h. SHAP1 (1 μM) or LL-37 (0.25 μM) was then added. Migration was monitored for up to 24 h. Same fields were photographed immediately after wounding and 24 h later, and representative images are shown (wound margin depicted as *white dotted line*) (**c**). Relative wound closure after 24 h of incubation was calculated as described in "Materials and methods" from micrographs similar to those shown in **c** (**d**). The results shown are combined from three independent experiments; *error bars* represent the mean ± SD

wound closure (Fig. 3c, d). Migration of cells into the wounded area was significantly increased in the presence of SHAP1 (1 μM) over migration in the presence of PBS within 24 h after wounding. Comparative analysis of SHAP1 and LL-37 revealed that SHAP1 was more effective at inducing in vitro wound closure than LL-37. SHAP1

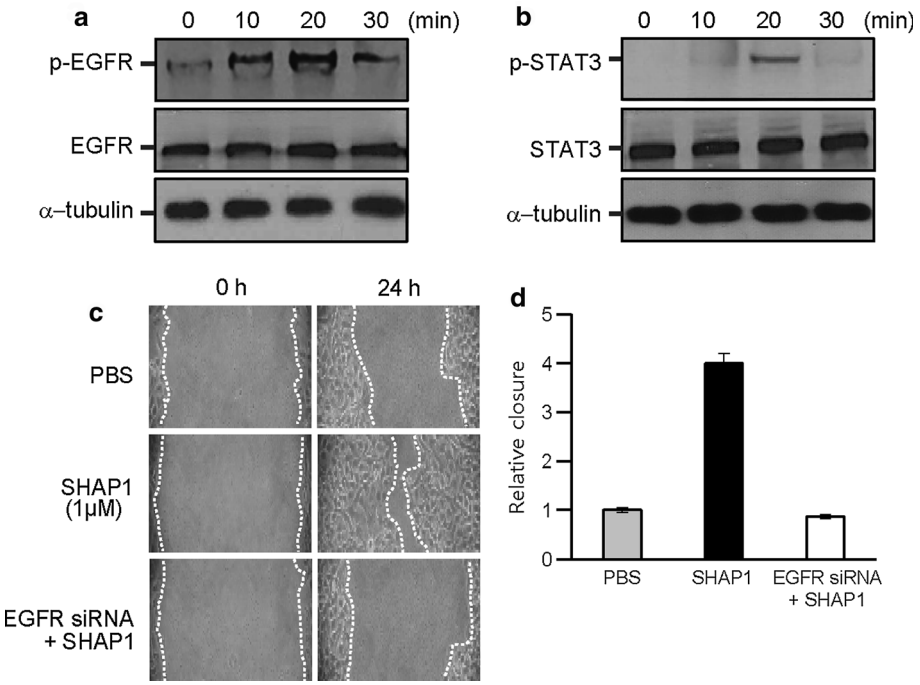

Fig. 4 SHAP1-induced wound closure via transactivation of EGFR. **a**, **b** EGFR and STAT3 phosphorylation in SHAP1-treated HaCaT cells. Subconfluent HaCaT cells were starved for 12 h in DMEM without 10 % FBS and stimulated with SHAP1 (1 μM). The cells were harvested into lysis buffer at the indicated times. The phosphorylation of EGFR (p-EGFR) and STAT3 (p-STAT3) was analyzed by Western blotting. EGFR and STAT3 indicate total EGFR and STAT3 protein, respectively. α-tubulin was used as the loading control. **c**, **d** Effect of EGFR silencing on SHAP1-induced wound closure. HaCaT cells were transfected with EGFR-specific siRNA. After 24 h, a scratch wound closure assay was performed. Same fields were photographed immediately after wounding and 24 h later, and representative images are shown (wound margin depicted as *white dotted line*) (**c**). Relative wound closure after 24 h of incubation with SHAP1 was calculated as described in "Materials and methods" from micrographs similar to those shown in **c** (**d**). The results shown are combined from three independent experiments; *error bars* represent the mean ± SD

(1 μM) was approximately two times more effective than LL-37 (0.25 μM) in promoting in vitro wound closure (4.1-fold increase with SHAP1 versus twofold with LL-37). There is minimal and no significant wound closure activity in the control treatment (PBS).

SHAP1-induced wound closure via transactivation of EGFR

In an effort to address the mechanism of action of SHAP1 in wound closure, we searched for a key signaling pathway of SHAP1. EGFR signaling pathway is a well-known factor involved in wound closure (Puddicombe et al. 2000; Tokumaru et al. 2005). EGFR signaling pathway initiates several signal transduction cascades, such as STAT3 and Akt with the functional consequence of enhanced cell migration (Andl et al. 2004; Oda et al. 2005). Therefore, we investigated whether SHAP1 could induce phosphorylation of EGFR and STAT3 in HaCaT cells. EGFR and STAT3 were phosphorylated 10–20 min after the addition of SHAP1 (1 μM) in HaCaT cells (Fig. 4a, b). These results demonstrate an important role of EGFR signaling pathway in SHAP1-induced wound closure. To further strengthen our results, we incubated HaCaT cells with EGFR-specific siRNA for 24 h before stimulation with SHAP1, and then, assessed in vitro wound closure. The knockdown of EGFR by siRNA was confirmed by Western blot with anti-EGFR antibody (data not shown). As expected, EGFR-specific siRNA completely blocked wound closure induced by SHAP1, indicating that SHAP1-induced wound closure is mediated by EGFR signaling pathway (Fig. 4c, d).

Efficacy of SHAP1 in vivo

To evaluate a potential clinical application of SHAP1, we first investigated the in vivo wound closure activity of SHAP1 in a mouse full-thickness skin wound model (Fig. 5). Full-thickness round wounds of 10 mm in diameter were made on the back of mice, and the kinetics of wound closure was evaluated by measurement of original wound area (%). SHAP1 (1 μM/wound) or LL-37

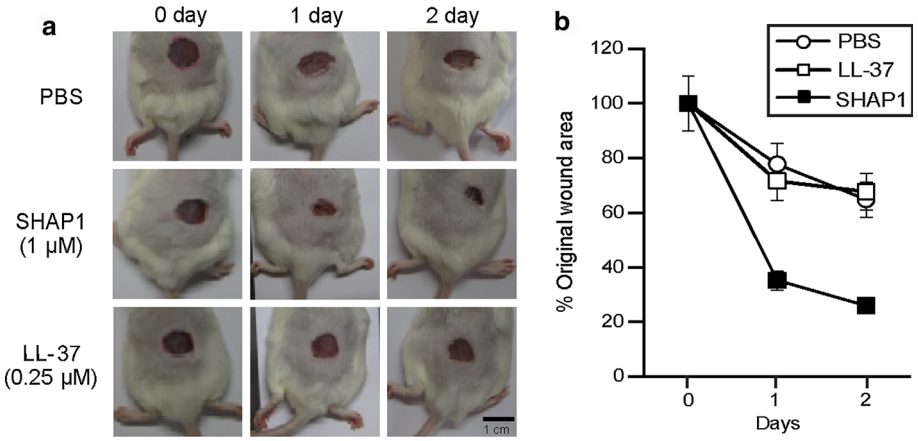

Fig. 5 Efficacy in wound healing of SHAP1 in a mouse full-thickness skin wound model. **a** Effect of SHAP1 on closure of full-thickness excisional wounds in mice. 10-mm-diameter excisions were made on the back of mice. Each wound was treated with SHAP1 or LL-37 every 24 h ($n = 5$ mice per group). The same animal was lightly anesthetized and photographed on the indicated days following injury. **b** Changes in percentage of wound area at each time point in comparison to the original wound area. Wound area was determined on photographs using Adobe Photoshop® v.5.0. Data are the mean ± SD of $n = 5$ and representative of two independent experiments

(0.25 μM/wound) was applied topically one time a day for 2 days post-injury, when a blood clot was generated. PBS was used as a control for the SHAP1 and LL-37 treatments. Wounds treated with SHAP1 were consistently smaller than wounds treated with PBS alone (Fig. 5a, b). The results showed that the difference in size was apparent at post-injury day 1, and by day 2 the wound treated with SHAP1 was smaller in area (26 % compared to original wound area) than the control wound (64.7 %). These results indicate that SHAP1 has accelerated skin wound closure and healing in mice. In contrast, there was no significant difference between LL-37- and PBS-applied wound areas in mice.

Most wounds are typically contaminated by bacteria. These infected wounds, in which bacteria or other microorganisms have colonized, cause either a delay in wound healing or deterioration of the wound (Chiller et al. 2001; Guay 2003). Therefore, we next sought to examine whether SHAP1 promotes wound closure and healing in a mouse wound infection model. Full-thickness round wounds (2 mm in diameter) were made on the back of mice, and subsequently inoculated with *S. aureus*. After treating the wounds with SHAP1 or PBS (control) every 24 h for 2 days, representative cross-sectional biopsies were taken to evaluate bacterial burden and wound histology (Fig. 6a, b). Bacterial counts were significantly reduced in the SHAP1-treated group (2.82 ± 1.16 log $_{10}$ CFU/g tissue) compared to the PBS-treated control group (7.02 ± 0.45 log $_{10}$ CFU/g tissue) ($p < 0.001$, SHAP1 versus PBS) (Fig. 6a). In addition, hematoxylin–eosin staining clearly demonstrated that SHAP1 led to an enhancement in wound closure compared to the PBS treatment (Fig. 6b).

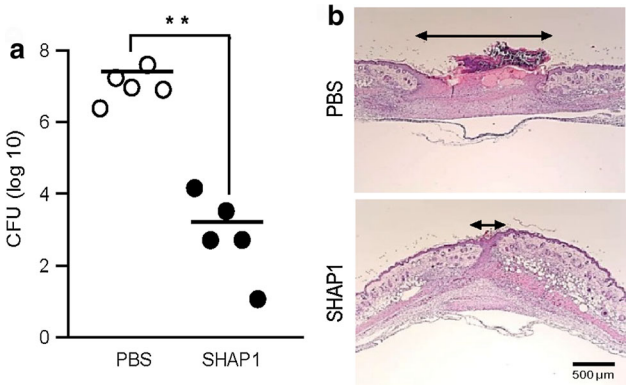

Fig. 6 Efficacy in wound healing of SHAP1 in a mouse wound infection model. **a** Assessment of bacterial colonization in *S. aureus*-infected wounds. 2-mm-diameter excisions were made on the back of mice. The wounds were infected with *S. aureus* for 24 h, followed by treatment with SHAP1 or PBS every 24 h. Wound tissue samples were harvested on day 3 after infection, and the number of CFU/g tissue was counted. *Each symbol* represents an individual mouse. The median value in each group is shown as a *horizontal bar* ($n = 5$; $^{**}p < 0.001$ versus PBS). **b** Histologic analysis of *S. aureus*-infected wounds. Sections from wound tissue samples harvested on day 3 after infection were stained with hematoxylin and eosin. *Black arrows* indicate epidermal gaps, which determine the degree of wound closure. Representative images from two independent experiments are shown

Discussion

Wound healing involves the precise orchestration of inflammation, epithelialization, tissue granulation and remodeling. Some AMPs, such as LL-37 and hBDs, are considered promising agents for wound care, because they influence all of these mechanisms in addition to their

intrinsic antimicrobial activities. Although the use of LL-37 and hBDs for the infected wound treatment is beginning to be explored (Jacobsen et al. 2005; Winter and Wenghoefer 2012), their therapeutic applications are limited due to their large size and sequence complexity (disulfide bridges of hBDs), and thus high associated manufacturing cost, as well as their toxicity and low stability in vivo (Marr et al. 2006; Hawrani et al. 2008; Kim et al. 2013). These setbacks led to increased efforts to develop short and compositionally simple synthetic peptides with desired characteristics: a broad-spectrum antimicrobial activity, low cytotoxicity, and strong wound closure activity that is capable of withstanding the host environment, including high salt concentration and proteases.

In this study, we have demonstrated that in addition to its previously reported antimicrobial activities, the designer peptide SHAP1 also possesses potent wound closure activities both in vitro and in vivo. SHAP1 was selected from a series of 32 synthetic AMPs because it showed potent antimicrobial activity against bacteria and fungi, and maintained their activity in the presence of 200 mM NaCl (Kim et al. 2008). SHAP1 did not affect the viability of human erythrocytes and keratinocytes up to 200 μM. SHAP1 elicited stronger wound closure activity than LL-37 in vitro by inducing HaCaT cell migration, which was shown to progress via transactivation of EGFR. SHAP1 phosphorylated EGFR and STAT3 in HaCaT cells, and the knockdown of EGFR by siRNA completely blocked wound closure induced by SHAP1 (Fig. 4). The mechanism through which SHAP1 transactivates EGFR is still unclear. Recently, it has been suggested that LL-37 activates a metalloproteinase, which cleaves the extracellular domain of heparin-binding EGF (HB-EGF). The soluble-form of HB-EGF then binds to and phosphorylates EGFR. This, in turn, transduces the signals into the intracellular signaling pathways mediated by STAT3, leading to keratinocyte migration (Tokumaru et al. 2005). It is postulated that the transactivation of EGFR by SHAP1, similar to LL-37, might be mediated by HB-EGF. Ongoing studies are aimed at dissecting the specific pathway involved in the transactivation of EGFR.

SHAP1 treatment accelerated closure and healing of full-thickness excisional wounds in mice. One of the important findings in this study is that SHAP1 exerted strong wound healing activities in vivo at the same low concentration (1 μM) that was used in in vitro assays. As shown in Fig. 5, topical application of SHAP1 (1 μM) accelerated closure and healing of full-thickness excisional wounds in mice. In contrast, there was no significant difference between LL-37- and PBS-applied wound areas in mice, though LL-37 (0.25 μM) exhibited in vitro wound closure activity. This result is most likely due to the fact that LL-37 was degraded by proteases in the wound site. It has been reported that more than 100 endogenous proteases are found in the wound fluid (Rawlings et al. 2010). Those proteases are more or less implicated in various phases of wound healing, and include matrix metalloproteases and neutrophil elastase (Gronberg et al. 2011; Stromstedt et al. 2009). In addition, many pathogenic bacteria, which contaminate wounds, secrete proteases such as *S. aureus* V8 proteinase. Accordingly, it has been suggested that the susceptibility of AMPs to proteolytic degradation by these proteases may pose a major limitation to their use as a human therapeutic modality for the infected wound treatment, although the peptides showed evidence of excellent in vitro antimicrobial and wound closure activities (Shin et al. 2010). Indeed, the protease resistance assay demonstrated that LL-37 was readily digested by neutrophil elastase and *S. aureus* V8 proteinase (Fig. 2). Therefore, high concentration of LL-37 might be required in vivo to attain the effective therapeutic concentration in the wound milieu full of these proteases. In contrast to LL-37, SHAP1 was completely resistant to proteolytic degradation by these proteases, which explains the reason that SHAP1 could promote wound healing in vivo at the same low concentration used in in vitro assays. Thus, from a therapeutic point of view, resistance of SHAP1 to proteases in the wound milieu could augment its therapeutic value for the infected wound treatment.

To study the wound healing properties of SHAP1 in a more complex wound environment, we examined the curative effect of SHAP1 in a *S. aureus*-infected wound model. Full-thickness round wounds were made on the back of mice, and subsequently inoculated with 5×10^5 CFU of *S. aureus*, which causes skin infections like folliculitis, boils, impetigo, and cellulitis. As shown in Fig. 6, topical application of SHAP1 (1 μM) resulted in significant decrease of bacterial counts in the wound tissue compared to PBS treatment. Histological analysis of SHAP1-treated wounds revealed an almost complete wound closure by day 3. These data indicated that SHAP1 effectively countered *S. aureus* infection and enhanced wound closure in this model, suggesting it may have clinical potential. We are now investigating the potential toxicity of SHAP1 by skin irritation and genotoxicity studies. Preliminary results showed that SHAP1 did not induce skin irritation in New Zealand white rabbits, and was non-genotoxic to mice (data not shown).

In conclusion, we have demonstrated that in addition to its previously reported salt-resistant antimicrobial activities, the designer peptide SHAP1 also possesses potent wound closure activities both in vitro and in vivo. SHAP1 promoted wound healing in both normal and infected wounds, and its effects were more potent than those of LL-37. Furthermore, SHAP1 did not affect the viability of human erythrocytes and keratinocytes, and was not

digested by human neutrophil elastase and *S. aureus* V8 proteinase. These features of SHAP1 suggest that SHAP1 might be developed as a novel topical agent for the infected wound treatment.

Acknowledgments This work was supported by the Intelligent Synthetic Biology Center of Global Frontier Project funded by the Ministry of Science, ICT & Future Planning (2011-0031955) and the Medicine & Bio Project for "New Drug Development through Fostering of Med-Bio Hub" of the Chungcheong Leading Industry Office (CCLIO) and Ministry of Knowledge Economy (MKE) (C2110907).

Conflict of interest The authors declare that they have no conflict of interest.

References

Andl CD, Mizushima T, Oyama K, Bowser M, Nakagawa H, Rustgi AK (2004) EGFR-induced cell migration is mediated predominantly by the JAK-STAT pathway in primary esophageal keratinocytes. Am J Physiol Gastrointest Liver Physiol 287: G1227–G1237

Baroni A, Donnarumma G, Paoletti I, Longanesi-Cattani I, Bifulco K, Tufano MA, Carriero MV (2009) Antimicrobial human beta-defensin-2 stimulates migration, proliferation and tube formation of human umbilical vein endothelial cells. Peptides 30:267–272

Bowler PG (2002) Wound pathophysiology, infection and therapeutic options. Ann Med 34:419–427

Carretero M, Del Rio M, Garcia M, Escamez MJ, Mirones I, Rivas L, Balague C, Jorcano JL, Larcher F (2004) A cutaneous gene therapy approach to treat infection through keratinocyte-targeted overexpression of antimicrobial peptides. FASEB J 18: 1931–1933

Carretero M, Escamez MJ, Garcia M, Duarte B, Holguin A, Retamosa L, Jorcano JL, Rio MD, Larcher F (2008) In vitro and in vivo wound healing-promoting activities of human cathelicidin LL-37. J Invest Dermatol 128:223–236

Chiller K, Selkin BA, Murakawa GJ (2001) Skin microflora and bacterial infections of the skin. J Investig Dermatol Symp Proc 6:170–174

Choi JH, Choi DK, Sohn KC, Kwak SS, Suk J, Lim JS, Shin I, Kim SW, Lee JH, Joe CO (2012) Absence of a human DnaJ protein hTid-1S correlates with aberrant actin cytoskeleton organization in lesional psoriatic skin. J Biol Chem 287:25954–25963

De Zotti M, Biondi B, Park Y, Hahm KS, Crisma M, Toniolo C, Formaggio F (2012) Antimicrobial lipopeptaibol trichogin GA IV: role of the three Aib residues on conformation and bioactivity. Amino Acids 43:1761–1777

Gopinath D, Kumar MS, Selvaraj D, Jayakumar R (2005) Pexiganan-incorporated collagen matrices for infected wound-healing processes in rat. J Biomed Mater Res A 73:320–331

Gronberg A, Zettergren L, Agren MS (2011) Stability of the cathelicidin peptide LL-37 in a non-healing wound environment. Acta Derm Venereol 91:511–515

Guay DR (2003) Treatment of bacterial skin and skin structure infections. Expert Opin Pharmacother 4:1259–1275

Hancock RE, Sahl HG (2006) Antimicrobial and host-defense peptides as new anti-infective therapeutic strategies. Nat Biotechnol 24:1551–1557

Hawrani A, Howe RA, Walsh TR, Dempsey CE (2008) Origin of low mammalian cell toxicity in a class of highly active antimicrobial amphipathic helical peptides. J Biol Chem 283:18636–18645

Jacobsen F, Mittler D, Hirsch T, Gerhards A, Lehnhardt M, Voss B, Steinau HU, Steinstraesser L (2005) Transient cutaneous adenoviral gene therapy with human host defense peptide hCAP-18/LL-37 is effective for the treatment of burn wound infections. Gene Ther 12:1494–1502

Jang SA, Kim H, Lee JY, Shin JR, da Kim J, Cho JH, Kim SC (2012) Mechanism of action and specificity of antimicrobial peptides designed based on buforin IIb. Peptides 34:283–289

Kim SC, Park IY, Kim JM (2008) Salt-resistant antimicrobial peptides and antimicrobial composition comprising thereof. Korea Patent 10-0836596

Kim H, Jang JH, Kim SC, Cho JH (2013) De novo generation of short antimicrobial peptides with enhanced stability and cell specificity. J Antimicrob Chemother. doi:10.1093/jac/dkt322

Koczulla R, von Degenfeld G, Kupatt C, Krotz F, Zahler S, Gloe T, Issbrucker K, Unterberger P, Zaiou M, Lebherz C, Karl A, Raake P, Pfosser A, Boekstegers P, Welsch U, Hiemstra PS, Vogelmeier C, Gallo RL, Clauss M, Bals R (2003) An angiogenic role for the human peptide antibiotic LL-37/hCAP-18. J Clin Invest 111:1665–1672

Lee PH, Rudisill JA, Lin KH, Zhang L, Harris SM, Falla TJ, Gallo RL (2004) HB-107, a nonbacteriostatic fragment of the antimicrobial peptide cecropin B, accelerates murine wound repair. Wound Repair Regen 12:351–358

Lipsky BA, Hoey C (2009) Topical antimicrobial therapy for treating chronic wounds. Clin Infect Dis 49:1541–1549

Ma QQ, Dong N, Shan AS, Lv YF, Li YZ, Chen ZH, Cheng BJ, Li ZY (2012) Biochemical property and membrane-peptide interactions of de novo antimicrobial peptides designed by helix-forming units. Amino Acids 43:2527–2536

Malmsten M, Kasetty G, Pasupuleti M, Alenfall J, Schmidtchen A (2011) Highly selective end-tagged antimicrobial peptides derived from PRELP. PLoS One 6:e16400

Marr AK, Gooderham WJ, Hancock RE (2006) Antibacterial peptides for therapeutic use: obstacles and realistic outlook. Curr Opin Pharmacol 6:468–472

McHugh SM, Collins CJ, Corrigan MA, Hill AD, Humphreys H (2011) The role of topical antibiotics used as prophylaxis in surgical site infection prevention. J Antimicrob Chemother 66:693–701

Mookherjee N, Hancock RE (2007) Cationic host defence peptides: innate immune regulatory peptides as a novel approach for treating infections. Cell Mol Life Sci 64:922–933

Mookherjee N, Brown KL, Bowdish DM, Doria S, Falsafi R, Hokamp K, Roche FM, Mu R, Doho GH, Pistolic J, Powers JP, Bryan J, Brinkman FS, Hancock RE (2006) Modulation of the TLR-mediated inflammatory response by the endogenous human host defense peptide LL-37. J Immunol 176:2455–2464

Myhrman E, Hakansson J, Lindgren K, Bjorn C, Sjostrand V, Mahlapuu M (2012) The novel antimicrobial peptide PXL150 in the local treatment of skin and soft tissue infections. Appl Microbiol Biotechnol 97:3085–3096

Niyonsaba F, Ushio H, Nakano N, Ng W, Sayama K, Hashimoto K, Nagaoka I, Okumura K, Ogawa H (2007) Antimicrobial peptides human beta-defensins stimulate epidermal keratinocyte migration, proliferation and production of proinflammatory cytokines and chemokines. J Investig Dermatol 127:594–604

Oda K, Matsuoka Y, Funahashi A, Kitano H (2005) A comprehensive pathway map of epidermal growth factor receptor signaling. Mol Syst Biol 1(2005):0010

Overhage J, Campisano A, Bains M, Torfs EC, Rehm BH, Hancock RE (2008) Human host defense peptide LL-37 prevents bacterial biofilm formation. Infect Immun 76:4176–4182

Park IY, Cho JH, Kim KS, Kim YB, Kim MS, Kim SC (2004) Helix stability confers salt resistance upon helical antimicrobial peptides. J Biol Chem 279:13896–13901

Pasupuleti M, Schmidtchen A, Chalupka A, Ringstad L, Malmsten M (2009) End-tagging of ultra-short antimicrobial peptides by W/F stretches to facilitate bacterial killing. PLoS One 4:e5285

Philp D, Badamchian M, Scheremeta B, Nguyen M, Goldstein AL, Kleinman HK (2003) Thymosin beta 4 and a synthetic peptide containing its actin-binding domain promote dermal wound repair in db/db diabetic mice and in aged mice. Wound Repair Regen 11:19–24

Puddicombe SM, Polosa R, Richter A, Krishna MT, Howarth PH, Holgate ST, Davies DE (2000) Involvement of the epidermal growth factor receptor in epithelial repair in asthma. FASEB J 14:1362–1374

Radek KA, Taylor KR, Gallo RL (2009) FGF-10 and specific structural elements of dermatan sulfate size and sulfation promote maximal keratinocyte migration and cellular proliferation. Wound Repair Regen 17:118–126

Rawlings ND, Barrett AJ, Bateman A (2010) MEROPS: the peptidase database. Nucleic Acids Res 38((Database issue)):D227–D233

Shaykhiev R, Beisswenger C, Kandler K, Senske J, Puchner A, Damm T, Behr J, Bals R (2005) Human endogenous antibiotic LL-37 stimulates airway epithelial cell proliferation and wound closure. Am J Physiol Lung Cell Mol Physiol 289:L842–L848

Shin YP, Park HJ, Shin SH, Lee YS, Park S, Jo S, Lee YH, Lee IH (2010) Antimicrobial activity of a halocidin-derived peptide resistant to attacks by proteases. Antimicrob Agents Chemother 54:2855–2866

Shin JR, Lim KJ, da Kim J, Cho JH, Kim SC (2013) Display of multimeric antimicrobial peptides on the Escherichia coli cell surface and its application as whole-cell antibiotics. PLoS One 8:e58997

Sieprawska-Lupa M, Mydel P, Krawczyk K, Wojcik K, Puklo M, Lupa B, Suder P, Silberring J, Reed M, Pohl J, Shafer W, McAleese F, Foster T, Travis J, Potempa J (2004) Degradation of human antimicrobial peptide LL-37 by Staphylococcus aureus-derived proteinases. Antimicrob Agents Chemother 48:4673–4679

Steinstraesser L, Koehler T, Jacobsen F, Daigeler A, Goertz O, Langer S, Kesting M, Steinau H, Eriksson E, Hirsch T (2008) Host defense peptides in wound healing. Mol Med 14:528–537

Steinstraesser L, Kraneburg UM, Hirsch T, Kesting M, Steinau HU, Jacobsen F, Al-Benna S (2009) Host defense peptides as effector molecules of the innate immune response: a sledgehammer for drug resistance? Int J Mol Sci 10:3951–3970

Stromstedt AA, Pasupuleti M, Schmidtchen A, Malmsten M (2009) Evaluation of strategies for improving proteolytic resistance of antimicrobial peptides by using variants of EFK17, an internal segment of LL-37. Antimicrob Agents Chemother 53:593–602

Tokumaru S, Sayama K, Shirakata Y, Komatsuzawa H, Ouhara K, Hanakawa Y, Yahata Y, Dai X, Tohyama M, Nagai H, Yang L, Higashiyama S, Yoshimura A, Sugai M, Hashimoto K (2005) Induction of keratinocyte migration via transactivation of the epidermal growth factor receptor by the antimicrobial peptide LL-37. J Immunol 175:4662–4668

Torpy JM, Burke A, Glass RM (2005) JAMA patient page. Wound infections. JAMA 294:2122

Winter J, Wenghoefer M (2012) Human defensins: potential tools for clinical applications. Polymers 4:691–709

Yin J, Yu FS (2010) LL-37 via EGFR transactivation to promote high glucose-attenuated epithelial wound healing in organ-cultured corneas. Invest Ophthalmol Vis Sci 51:1891–1897